Ecological Indicators 107 (2019) 105595

Contents lists available at ScienceDirect

Ecological Indicators

journal homepage: www.elsevier.com/locate/ecolind

Original Articles

# Assessing land degradation and quantifying its drivers in the Amudarya River delta

Liangliang Jiang[a,b,c,d,e,f], Guli Jiapaer[a,b,c,e], Anming Bao[a,b,c,e,*], Yaoming Li[a,c], Hao Guo[a,b,c,e,f], Guoxiong Zheng[a,b,c], Tao Chen[a,b,c], Philippe De Maeyer[d,e,f]

[a] State Key Laboratory of Desert and Oasis Ecology, Xinjiang Institute of Ecology and Geography, Chinese Academy of Sciences, Urumqi 830011, China
[b] Key Laboratory of GIS & RS Application Xinjiang Uygur Autonomous Region, China
[c] University of Chinese Academy of Sciences, Beijing 100049, China
[d] Department of Geography, Ghent University, Ghent 9000, Belgium
[e] Sino-Belgian Joint Laboratory of Geo-information, Urumqi 830011, China
[f] Sino-Belgian Joint Laboratory of Geo-information, Ghent 9000, Belgium

ARTICLE INFO

*Keywords:*
Land degradation
Climate change
Anthropogenic disturbances
Amudarya River delta

ABSTRACT

The shrinking of the Aral Sea is one of the most shocking environmental disasters in the world. The Amudarya River delta (AD) is highly vulnerable to land degradation. In this research, NDVI and albedo, which represent vegetation and soil conditions, were applied in change vector analysis (CVA) to monitor land degradation. The vegetation degradation and soil exposure characteristics of land degradation were considered. Furthermore, based on boosted regression trees (BRTs), eight potential driving factors (precipitation, temperature, drought, water withdrawal, canal, livestock, salt discharge and population) were chosen to explore their relative importance to land degradation. The results revealed that some land areas have gradually degraded and fell into high land degradation in the AD, especially in the downstream areas near the Aral Sea. Soil salinization is a major consequence of high land degradation in this region. Subsequently, 920.75 $km^2$ and 183.10 $km^2$ of abandoned croplands were converted to sparse vegetation and grasslands, respectively. The BRT model indicated that water withdrawal availability and decreased precipitation were the most influential factors explaining the land degradation of croplands and natural vegetation from 1990 to 2000, respectively. In contrast, the salt discharge to the field plot was a major force causing land degradation of different vegetation types in the subsequent time interval (2000–2015). Because an increase in the groundwater level resulted in secondary soil salinization, a large proportion (45%) of the increased salinization occurred during this time period. Notably, due to the accelerated shrinking of the Aral Sea, some land areas surrounding the sea have fallen into high land degradation. Our findings can contribute to the implementation of the land degradation neutrality initiative to deploy restoration plans in the AD.

## 1. Introduction

The Aral Sea was once the fourth largest inland lake in the world, providing a wealth of important ecosystem services and biodiversity (Micklin et al., 2016b). Currently, the Aral Sea basin is one of the world's major cotton producers (White, 2013). However, the shrinking of the Aral Sea due to extensive agricultural expansion is one of the most shocking environmental disasters in the world. As a result, the ecosystems surrounding the Aral Sea have been nearly destroyed, and the hydrological balance of the area has changed, particularly in the Amudarya River delta (AD) (Khamzina et al., 2008). This region (characterized by a fragile ecological environment) has suffered from vegetation degradation, soil salinization, dust storms and climate change at the former shoreline (Micklin, 2007). Land degradation in the AD has become a prominent environmental issue in recent decades (Asarin et al., 2010).

Currently, land degradation is one of the greatest ecological issues throughout the world and will worsen without rapid remedial actions (IPBES, 2018; UNCCD, 2017). One-third of the global land area is threatened by the effects of land degradation, which relates to 20% of the global population, especially rural communities in poverty (UNCCD, 2017). The ecological environmental problem is particularly

* Corresponding author at: State Key Laboratory of Desert and Oasis Ecology, Xinjiang Institute of Ecology and Geography, Chinese Academy of Sciences, Urumqi 830011, China.
*E-mail address:* baoam@ms.xjb.ac.cn (A. Bao).

https://doi.org/10.1016/j.ecolind.2019.105595
Received 18 May 2019; Received in revised form 22 July 2019; Accepted 25 July 2019

severe in drylands, which cover approximately 45% of the world's land surface, and the problem is continuously worsening and threatens more than 2 billion people (Prăvălie, 2016; Prăvălie et al., 2019a; Reynolds et al., 2007). Land degradation in the AD is a notable case related to water shortages. However, land degradation in this region is not well understood.

Land degradation can be triggered by anthropogenic disturbances and climatic variations (UNCCD, 1994). Anthropogenic disturbances have been shown to have obvious regional characteristics in the AD. Due to the expansion of irrigation in upstream areas, agriculture (in the AD) has faced serious water shortages in dry years. Furthermore, the salt discharge that reaches the delta has increased because of the salt leaching from the upstream regions of the river (Bank, 1998). These saline flows result in land degradation, and in conjunction with inadequate and inefficient irrigation water use, they could augment the groundwater tables and promote secondary soil salinization. Additionally, because of the accelerated shrinking of the Aral Sea, the climate has changed along the former coastline. Maritime regions have been replaced by sparse vegetation. The AD has become warm in summer and cool in winter with low humidity (Micklin, 2007). Moreover, the large climate fluctuations in the Amudarya River basin are a driver of runoff change and will affect the water withdrawal availability for agriculture, particularly in the AD (Stulina and Eshchanov, 2013). The rich and diverse ecosystems in these regions have suffered from considerable harm under extensive human activities and climate change, especially in the area surrounding the Aral Sea (Fig. 1) (Micklin, 2004). However, the monitoring of land degradation in this region, along with different driving factors, has received little attention.

Land degradation has been studied via different methodologies by means of various indicators on regional scales (Dubovyk et al., 2013a; Liu et al., 2018; Vogt et al., 2011; Zhang et al., 2017). Currently, the normalized difference vegetation index (NDVI) and albedo have been widely used to monitor land degradation (Karnieli et al., 2014; Kundu and Dutta, 2011; Li et al., 2016; Ma et al., 2011). Reduction in vegetation cover is a good indicator of vegetation degradation for monitoring leaf area index and green biomass reduction (Kundu and Dutta, 2011). Albedo is an important physical parameter that reflects soil characteristics. Surface albedo is closely related to soil moisture and soil exposure (Röder and Hill, 2009). Increased albedo can be used as an indirect indicator for the detection of soil degradation in arid regions (Liu et al., 2017; Mariano et al., 2018). Previous studies have contributed to the development of land degradation assessments by coupling NDVI and albedo using remote sensing data. However, more publications have focused on land degradation than on the responses to the underlying explanatory factors (Liu et al., 2018; Pan and Li, 2013; Vorovencii, 2017). It is critical to deeply understand the driving factors to prevent land degradation posed by human pressure and climatic variations. In addition, the assessment of land degradation in most studies did not consider the characteristics of different vegetation types when determining the relative importance of the driving forces (Li et al., 2016; Zhou et al., 2015). Anthropogenic activities have different influences on crops and natural vegetation in the AD. Thus, the consideration of various vegetation types is essential in this research. Additionally, land degradation is a complicated process that includes land cover conversions (Gebremicael et al., 2018; Zhang et al., 2017). The combination of indicators and land use data would be more reasonable for monitoring land degradation.

The Aral Sea was divided into large and small lakes in 1987. The large and small lakes receive water from the Amu Darya and the Syr Darya, respectively. A river flows from the small lake to the large lake. To restore the small Aral Sea, a 13 km dike was built to restrict the flow and protect the small Aral Sea (Micklin, 2007). Although the water level in the small lake has been maintained and has even increased in wet years, the land degradation in the AD (near the large Aral Sea) has worsened. Thus, it is necessary to assess land degradation and explore the driving forces. Vegetation degradation and soil exposure were considered land degradation in this study (Mariano et al., 2018). The regions with land degradation were identified as areas with decreased NDVI and increased albedo. The objectives of this research are to (1) monitor the spatial and temporal patterns of land degradation; (2) explore the spatial and temporal patterns of soil salinization; (3) investigate land use change and climate change; and (4) identify the relative importance of the driving factors of land degradation. Finally, the land degradation related to the major drivers at various time intervals

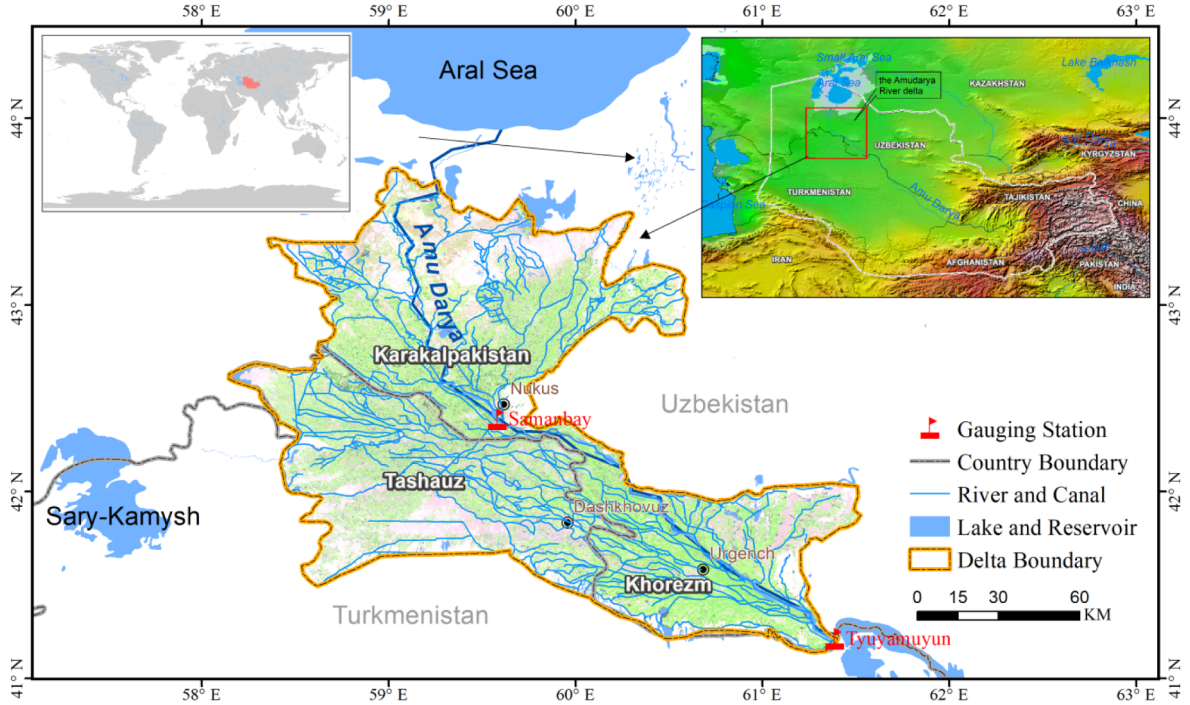


**Fig. 1.** Location map of the Amudarya River delta. National boundary data were acquired from the National Administration of Surveying, Mapping and Geoinformation with No. GS (2016) 1665.

was discussed. Hopefully, knowledge of the spatiotemporal features of land degradation will contribute to maintaining ecosystem services and preserving the ecological environment in the AD.

## 2. Materials and methods

### 2.1. Study area

The AD is located in the downstream region of the Amudarya River basin and comprises two provinces (Karakalpakistan and Khorezm) in Uzbekistan and one province (Tashauz) in Turkmenistan (Fig. 1). The AD spans from the Tyuyamuyun reservoir in the south to the Aral Sea in the north and from the Kyzylkum Desert in the east to the Ustyurt Plateau in the west, with an area amounting to 36,000 $km^2$. Large permanent glaciers and snow areas are distributed in the high Pamir mountains and feed the Amudarya River, which is a main source of water in the Amudarya River basin (Lee and Jung, 2018). As an end-water intake from the Amudarya River, the AD has been severely influenced by large-scale changes in the hydrological regime (Schlüter et al., 2013).

The region borders the Kyzylkum and Karakum deserts in the east and south, respectively, and belongs to the Central Asian semi-desert zone, which is characterized by an extreme continental climate with low precipitation and high irradiance (Khamzina et al., 2008). The mean annual precipitation varies from 80 to 120 mm/year. The amount of evapotranspiration greatly exceeds the mean annual precipitation. Evaporation is so high (approximately 1500 mm/year) because of the high winds and temperatures in summer (Akhtar et al., 2013; Schlüter et al., 2013). Therefore, most regions suffer from negative hydrological balances and depend on the freshwater inflow from the river (Lal et al., 2007), especially for irrigated agriculture, which is the backbone of the regional economy (Conrad et al., 2014).

The ecological environment in the AD is vulnerable to changes in the hydrological regime and human activities. The hydrological regime has been transformed dramatically due to cropland expansion, with a well-known impact on the deltaic ecological environment during the Soviet Union (Asarin et al., 2010; Micklin, 2007). Many regions have experienced land degradation and have been converted to sparse vegetation with the disappearance of grasslands and lakes (Dubovyk et al., 2016; Saiko and Zonn, 2000). However, after the Soviet Union collapsed, the river inflow into the AD became highly fluctuant and varied from 47.18 $km^3$ in 1998 to 10.47 $km^3$ in 2001, which was related to the extensive irrigation and water regulation in the upstream regions (Schettler et al., 2013). Moreover, conflicts over water allocation have occurred between the water management administration and water use sectors, as well as between the upstream and downstream regions in the AD. The irrigation needs for agriculture often conflict with the ecological water demands of natural ecosystems. In addition to the water deficit, this area is well known for its severe soil salinization. Virtually, most croplands in the region are subject to various degrees of soil salinity as a result of shallow saline groundwater tables, leading to land degradation (Dubovyk et al., 2013b; Khamzina et al., 2008). Therefore, the assessment of land degradation is essential in the AD.

### 2.2. Data sources

The datasets used in the study include Landsat image data, land use data and some driving factor data.

The Landsat images (TM, ETM + and OLI) were chosen to build three mosaics for 1990, 2000 and 2015 at a spatial resolution of 30 m. Five scenes (path/row 159/31, 160/30, 160/31, 161/30 and 161/31) were acquired to cover the entire study area. The Landsat data were downloaded from the United States Geological Survey (http://glovis.usgs.gov/). To consider the fact that the annual image phase cannot be exactly the same, these time-series data were employed from May to September in each period. Due to the limits of clouds and temporal resolution in the given year, some Landsat data (stemming from earlier or later years) were applied to build a cloudless image that covered the entire study area. Finally, 82 cloud-free Landsat images were selected in the study.

The land use data were provided by the Research Centre for Ecology and Environment of Central Asia at the Chinese Academy of Sciences and were interpreted based on the Landsat images from 1990, 2000 and 2015, along with the corresponding land degradation information. Land use/cover types were divided into six first-level types (cropland, forest, grassland, wetland, built-up land and sparse vegetation) with high accuracy (Chen et al., 2015).

To identify the relative importance of the explanatory factors for land degradation, the potential explanatory variables were chosen to consider climate change and human activities according to the definition of land degradation implemented by the United Nations Convention to Combat Desertification (UNCCD). Considering the data availability and region-specific environmental characteristics, eight key potential explanatory variables (precipitation, temperature, drought, water withdrawal, canal, livestock, salt discharge and population) were selected in this study (Table S1, Supplementary Material).

The global gridded precipitation and temperature data were obtained from the Climatic Research Unit Datasets from 1990 to 2015. The gridded climate data were generated based on the observation station data. This dataset possesses good quality control (Mitchell and Jones, 2005). The drought information was acquired from the global Standardized Precipitation Evapotranspiration Index (SPEI) database (http://spei.csic.es/database.html). The annual statistical data on water withdrawal and salt discharge were derived from the Database of the Amudarya River Basin provided by the Interstate Commission for Water Coordination of Central Asia from 1990 to 2015 (http://www.cawater-info.net/). The information on the other data is provided in Table S1. The soil salinization data were calculated based on the Landsat data. The inversion model has been verified in previous studies (Bouaziz et al., 2011; Gorji et al., 2017). The formula used to calculate the salinity index (SI) is as follows (Bouaziz et al., 2011):

$$SI(TM/ETM) = \sqrt{\alpha_1 \times \alpha_3} \quad (1)$$

$$SI(OLI) = \sqrt{\alpha_2 \times \alpha_4} \quad (2)$$

where $\alpha_1$, $\alpha_2$, $\alpha_3$ and $\alpha_4$ illustrate the reflectance in the corresponding spectral bands from the Landsat spectral bands.

### 2.3. Methods

#### 2.3.1. Change vector analysis

The change vector analysis (CVA) method is widely applied to monitor ecosystems and to research land change dynamics (Salih et al., 2017; Vorovencii, 2017). CVA is a change-detection technique that focuses on the magnitude and direction of changes in the multitemporal space among remote sensing images (Lambin and Strahlers, 1994). In this research, the NDVI and albedo pairs were applied in CVA to monitor land degradation, which represent the vegetation and soil conditions, respectively (Liu et al., 2018; Vorovencii, 2017).

The NDVI is related to various vegetation parameters, such as biomass productivity and leaf area index (Zaady et al., 2007). Negative changes in the NDVI values indicate an increase in vegetation degradation. The NDVI was calculated according to the reflectance of the red (R) and near-infrared (NIR) bands of a Landsat image (Rouse et al., 1974).

Albedo is a key physical parameter that reflects land surface conditions, including soil moisture and soil exposure (Röder and Hill, 2009). A positive change in the albedo values indicates an increase in soil degradation (Ma et al., 2011). In this study, the land surface albedo was measured based on the spectral bands of Landsat data (Liang, 2001). The formula for albedo based on TM/OLI data is as follows:

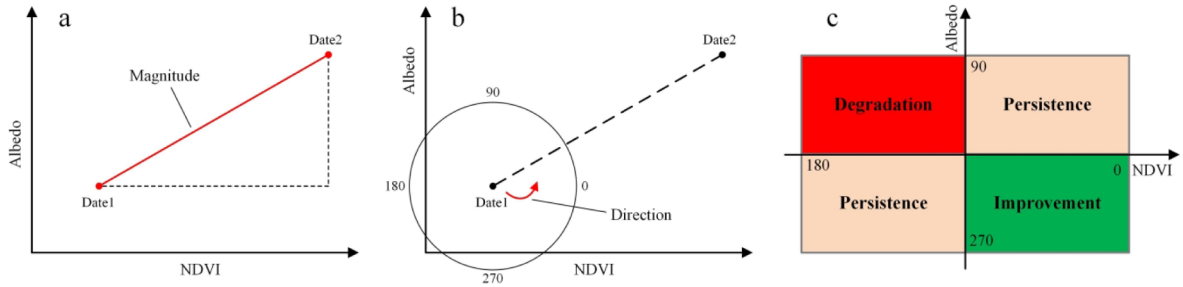


**Fig. 2.** The diagrams of the change vector analyses. (a) Change magnitude; (b) change direction; (c) change classified into three classes.

$$Albedo\ (TM/ETM) = 0.356\alpha_1 + 0.130\alpha_3 + 0.373\alpha_4 + 0.085\alpha_5 + 0.072\alpha_7 - 0.0018 \quad (3)$$

$$Albedo\ (OLI) = 0.356\alpha_2 + 0.130\alpha_4 + 0.373\alpha_5 + 0.085\alpha_6 + 0.072\alpha_8 - 0.0018 \quad (4)$$

where $\alpha_1$, $\alpha_2$, $\alpha_3$, $\alpha_4$, $\alpha_5$, $\alpha_6$, $\alpha_7$ and $\alpha_8$ demonstrate the spectral reflectance of the corresponding spectral bands of the Landsat TM/ETM and OLI images.

The magnitude (ΔM) of the changes in CVA represented the intensity of change between date 1 and date 2 based on the Euclidian distance (Fig. 2a). The ΔM values can be categorized to identify the degrees of land degradation or improvement. This value was calculated as follows (Dawelbait and Morari, 2012):

$$\Delta M_{band1\_band2} = \sqrt{(date2band1 - date1band1)^2 + (date2band2 - date1band2)^2} \quad (5)$$

where date2band1 represents the value of the NDVI on date 2, and date2band2 represents the value of the albedo on date 2.

The direction of the change was measured as the angle (α) between the two indicators, which represents the change from one pixel calculated on date 1 to the corresponding pixel measured on date 2 (Fig. 2b). The angle is acquired by applying the following formula (Dawelbait and Morari, 2012):

$$tg\alpha_{band1\_band2} = \frac{date2band2 - date1band2}{date2band1 - date1band1} \quad (6)$$

The direction of the change is categorized as four quadrants (Fig. 2c). In the first quadrant (0°–90°) and the third quadrant (180°–270°), the result shows an increase and decrease in both components, respectively, indicating persistent land conditions. In the second quadrant (90°–180°), the result illustrates that the NDVI is negative and the albedo is positive, indicating that the areas with land degradation were considered. In the fourth quadrant (270°–360°), the NDVI is positive and the albedo is negative, representing that the areas with land improvement were taken into consideration.

### 2.3.2. Boosted regression trees

In this study, the influence of the explanatory factors on land degradation was quantified using the boosted regression tree (BRT) model. The BRT model is a machine learning model that utilizes a non-parametric regression technique combined with the contribution of the explanatory factors (Elith et al., 2008). The modelling of natural phenomena with complicated non-linear relations has been advanced from a technical perspective via the use of BRTs. These models can automatically solve the interaction effects without requiring the prior transformation of explanatory data (Elith et al., 2008). Two algorithms were used in the BRTs: boosting and regression trees. Regression trees have several other advantages. This method can modify the missing values in the explanatory variables and is not sensitive to irrelevant input variables. Due to its easy implementation, interpretation and visualization, regression trees have become a popular technique (Hastie et al., 2015). Compared with single tree models with relatively poor prediction performance, boosting is used in BRTs to establish highly precise rules and to improve the model accuracy (Schapire, 2003). Because subsamples were chosen randomly at each iteration, the BRT approach is robust and not prone to overfitting (Friedman, 2002). The combination of good interpretability of the variables and high predictive accuracy is another particular advantage of BRTs (Friedman, 2001). Therefore, the BRT method has been broadly applied in remote sensing and land use change studies (Müller et al., 2013; Naghibi et al., 2016; Sica et al., 2016). A more comprehensive explanation of BRTs is provided in the study of Elith et al. (2008).

The BRT model was implemented in R using the code from the "dismo" package (Hijmans and Elith, 2013). Three main parameters need to be specified in the model: (1) learning rate, (2) tree complexity and (3) bag fraction. All combinations of learning rates from 0.1 to 0.0001 and tree complexities from 1 to 10 were tested to determine the optimal parameters according to the lowest prediction error. The result indicated that a learning rate of 0.01, a tree complexity of 5 and a bagging fraction of 0.5 fit the model with high predictive accuracy. According to both the improvement to the model when the explanatory factor is included and the frequency in which the factor is selected, the relative importance of the explanatory factors is estimated in the BRT. Finally, to understand the relationship between land degradation and each explanatory factor, we used partial dependence plots. The partial dependence plots demonstrate the contribution of each factor to land degradation after considering the equal influences from other factors.

For input data with the same spatial resolution, we resampled the spatial resolution of the explanatory factor data to a medium spatial resolution of 1/12° and composed yearly data. Thus, the output data shown in the partial dependence plots were counted from the BRT model based on the spatial resolution of 1/12°.

### 2.3.3. Mann–Kendall test

To identify the sub-time periods for exploring the direction of land degradation, the mutation years were detected using the Mann–Kendall (MK) test in this study. Currently, the MK test has been robustly used in hydrological and meteorological studies (Bandoc and Prăvălie, 2015; Prăvălie et al., 2016, 2019b; Su et al., 2014). The detailed process of the MK test can be referenced in previous studies (Mann, 1945; Sneyers, 1991).

## 3. Results

### 3.1. Spatiotemporal assessment of land degradation

The river runoff variation in the AD has been attributed to climate change and the expansion of water withdrawals for agriculture by human activities in the upstream areas. Thus, the annual precipitation, temperature and runoff were selected to observe the mutation years to determine different time intervals based on the MK test (Fig. 3). Most points intersected the 95% confidence intervals in approximately 2000, which indicates that 2000 can be considered the mutation year from 1990 to 2015. Two time intervals (1990–2000 and 2000–2015) were chosen for further analysis of land degradation.

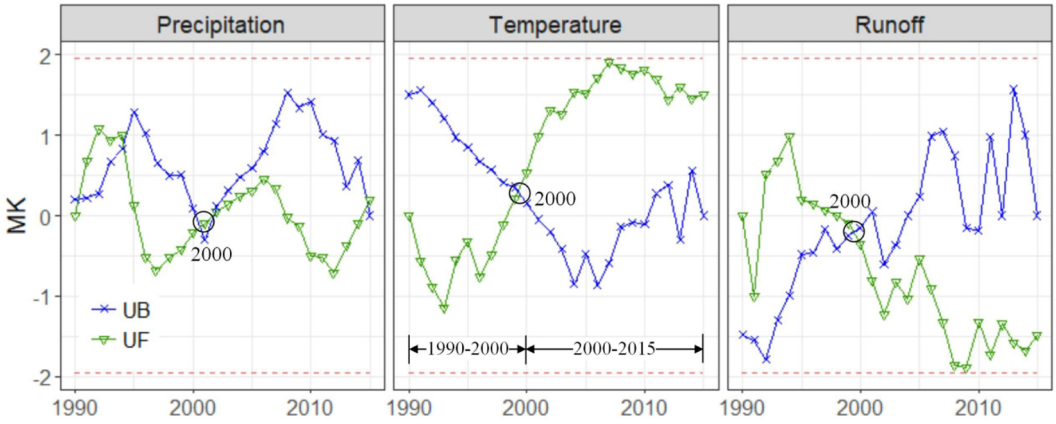


**Fig. 3.** Mutation results of the annual precipitation, temperature and runoff in the AD. The two red dotted lines are the two critical lines ( ± 1.96).

The spatial distribution of land degradation and improvement as shown in Fig. 4. There were spatial and temporal features of both land degradation and improvement in the AD from 1990 to 2015. In the study period (1990–2015), low negative values were observed in the southwestern part of Tashauz Province, with magnitude values as low as −0.38. Moreover, the high values were especially concentrated in the downstream areas in northern Karakalpakistan Province, with magnitude values amounting to 0.38. For 1990–2000, high positive values were noted in the northern part of the AD, showing land degradation, while low negative values were observed in the southern part of the AD, indicating land improvement. Opposite spatial changes were also identified between the northern part (the negative values) and the southern part (the positive values) from 2000 to 2015. However, some regions around the Aral Sea underwent severe degradation and should not be ignored. In general, large scattered areas with land degradation were detected in the downstream areas, while concentrated areas with land improvement were found in southwestern Tashauz Province. Thus, land degradation in the AD demonstrates significant regional characteristics.

Based on Landsat images, three regions were chosen with vegetation degradation and soil exposure from 1990 to 2015 (Figs. S1 and S2, Supplementary Material). Land degradation in these areas was detected effectively by applying CVA to NDVI and albedo (Fig. S2, Supplementary Material). Thus, the result of the CVA method is reliable for land degradation monitoring.

Considering the different degrees of the intensity of land degradation or improvement, the threshold value between the low and high change intensities was determined based on the density curve of the magnitude (ΔM) of the changes (Fig. S3, Supplementary Material). Because the intensity of change has two classes (low and high), the threshold was defined by the tails of a 50% distribution (Fig. S3, Supplementary Material). Then, by combining the results of the direction of change according to CVA (Fig. 2), the degrees of the intensity of change could be classified into four categories (Table 1). Fig. 4f demonstrates that the change intensity in the AD is spatially inconsistent from 1990 to 2015 and that high land improvement was found in the southwestern part. However, high land degradation was observed in the downstream areas. Most of the lands experienced high or low degradation (39.34%), while some lands underwent high or low improvement (22.53%). Furthermore, 38.13% of the areas were identified as persistent regions. Concerning the high land degradation, a higher percentage (15.37%) was observed for 2000–2015 than for 1990–2000. In terms of the percentage of persistent land, there were noteworthy decreases during different time periods, with 39.26% of the pixels being categorized as persistent land from 2000 to 2015. Overall, one can conclude that some lands were gradually degraded and fell into high land degradation in the AD, especially in the downstream areas next to the Aral Sea.

The results of the percentage changes of five classes for the different provinces are shown in Fig. 5, and the land degradation in different time intervals varied among the three provinces. From 1990 to 2000, higher percentages of land degradation were found in Karakalpakistan Province than in the other provinces (Fig. 5), where 17.66% and 23.19% of the pixels demonstrated high and low land degradation, respectively, followed by those in Tashauz Province. A large proportion of land improvement was identified in Khorezm Province. Khorezm Province accounted for 15.27% and 20.16% of the pixels with high and low land improvement, respectively. However, from 2000 to 2015, the proportions of high and low land degradation in Khorezm Province were 14.08% and 20.19%, respectively, and these values were greater than those in the first interval. Moreover, the proportion of land improvement from 2000 to 2015 has declined rapidly compared with that from 1990 to 2000. In the entire study period, the proportion of land degradation for the different provinces decreased in the following order: Karakalpakistan Province, Tashauz Province and Khorezm Province. The downstream areas were more likely to be degraded.

### 3.2. Spatiotemporal assessment of soil salinization

Based on the Landsat data, the SI was calculated and the spatial distribution of the soil salinization is displayed in Fig. 6. We found that the soil salinization in the AD was more serious in 2000–2015 than in 1990–2000. Increased salinization was concentrated in the downstream areas from 2000 to 2015, with increased SIs up to 0.12, while decreased salinization was identified in the southwestern AD in this period, with decreased SIs as low as −0.13. However, different spatial changes were also found in the first time interval (1990–2000). Most areas with decreased salinization occurred in the northern part of the AD. The results indicated that some influencing factors of soil salinization may be changed, leading to different land degradation trends for these two time intervals, especially in the northern AD.

The intensity of the soil salinization is categorized into five classes based on the density curve of the SI changes, which is the same as the classification method for land degradation (Table S2, Supplementary Material). The result reveals that the soil salinization change in the AD was not uniform in space and time from 1990 to 2015. For 1990–2000, most of the land experienced high or low decreased salinization (43%), while some land underwent high or low increased salinization (28%). Moreover, 29% of the areas were identified as persistent regions. However, opposite spatial changes in salinization were identified over the subsequent time interval (2000–2015). Twelve percent and 33% of the pixels showed high and low increased salinization, respectively. High increased salinization was observed in the downstream areas. Concerning decreased salinization, the proportions of high or low decreased salinization amounted to 29%, which was less than that in 1990–2000. Persistent regions accounted for 26% of the pixels. In

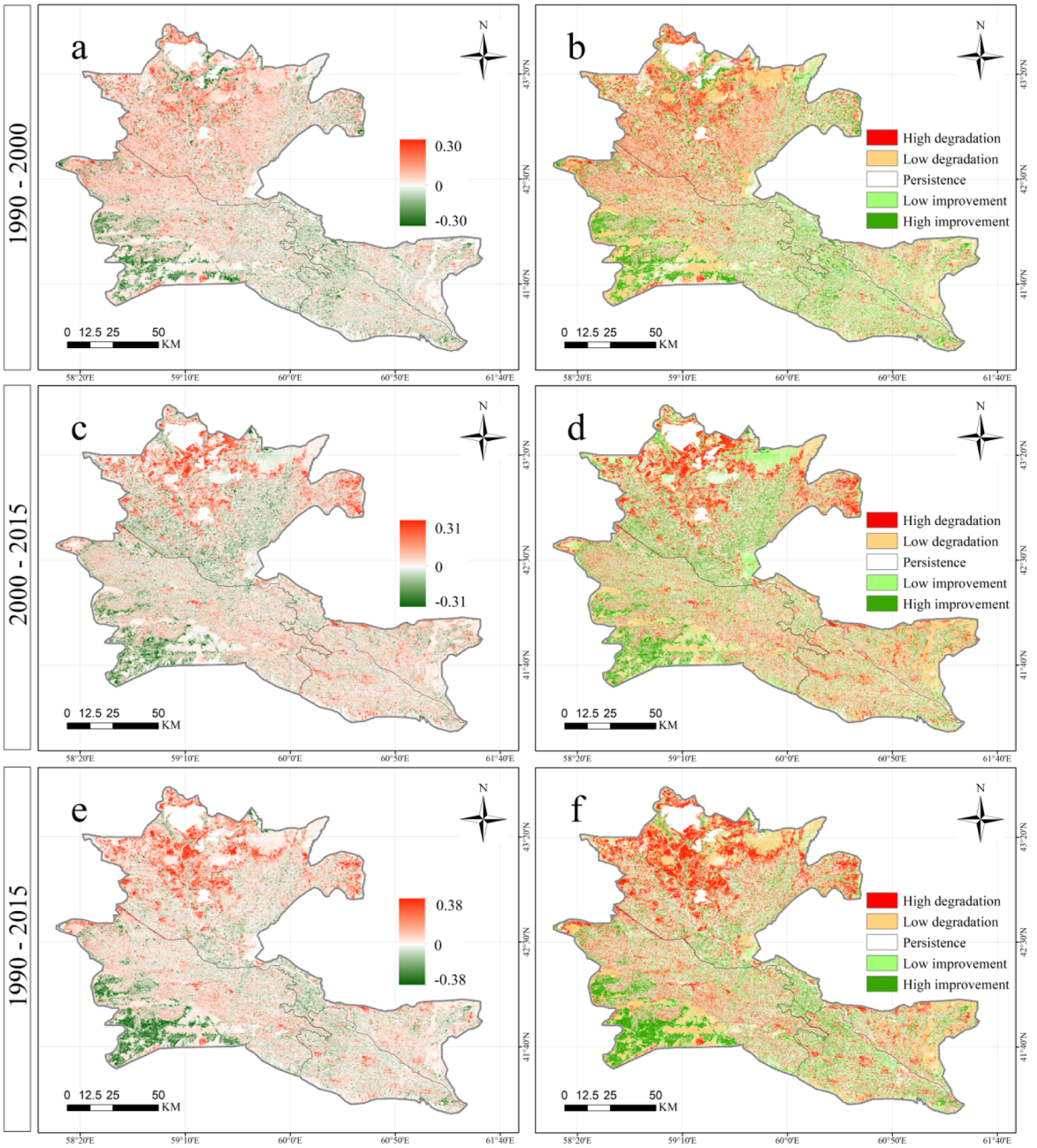


**Fig. 4.** Spatial distribution of land degradation and land improvement from 1990 to 2015. (a), (c) and (e) spatial distribution of the intensity of change according to CVA between different periods; (b), (d) and (f) the intensity of change classified into five classes of high degradation, low degradation, persistence, low improvement and high improvement.

**Table 1**
Degrees for division of the intensity of change according to CVA.

| ΔM | Land status classification |
|---|---|
| ≥0.1 | High vegetation degradation or improvement |
| 0–0.1 | Low vegetation degradation or improvement |

general, the soil salinization in most of the regions was more serious from 2000 to 2015 than from 1990 to 2000. Moreover, the degree of soil salinization in northern Karakalpakistan Province was higher than that in other areas.

### 3.3. Land use change from 1990 to 2015

Fig. 7 displays the land use maps for 1990, 2000 and 2015. These land use maps indicated that croplands were the dominant land use type in the AD in both periods. Table 2 demonstrates the statistical results for the different land use types and shows that the proportions of land use types varied over time. Croplands increased quickly from 48.14% in 1990 to 53.14% in 2000, while they decreased to 50.74% in 2015. The change in croplands led to spatial changes in water use, resulting in land degradation in the downstream areas. Concerning grasslands, the maximum percentage (22.35%) was observed in 1990. After that, almost 1852.68 $km^2$ of the grassland areas fell into other land use types, which were relatively concentrated in the northern part of the AD. For sparse vegetation, the area decreased by 227.96 $km^2$

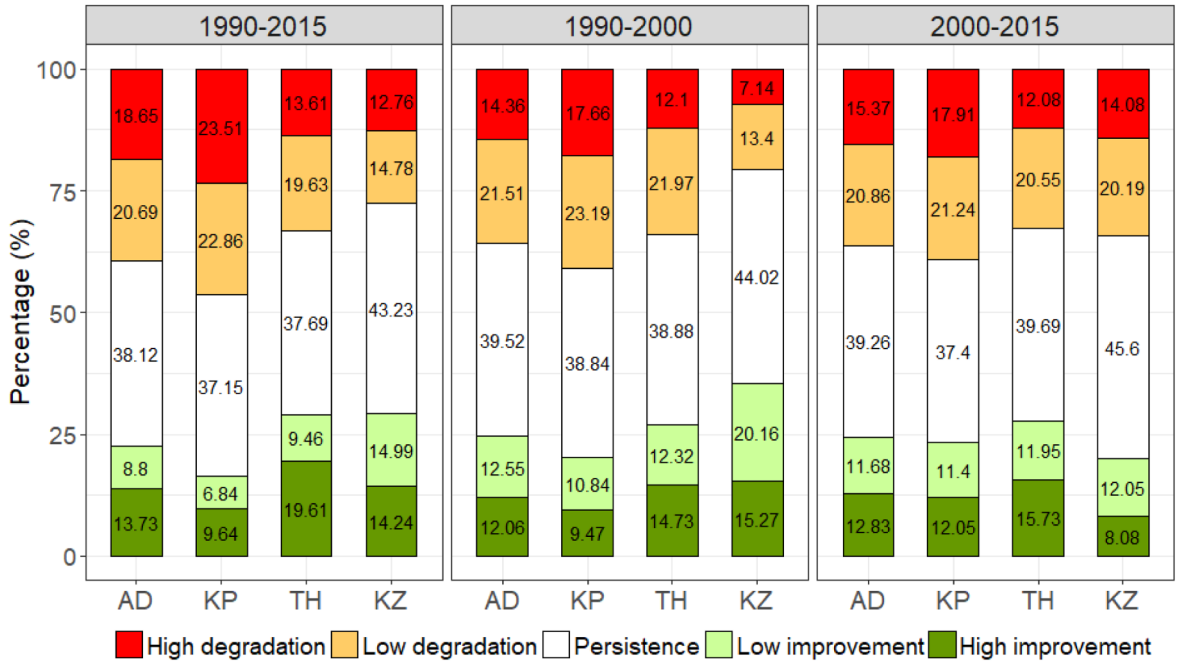


**Fig. 5.** The percent changes in five land status classes for different regions and time intervals. AD: Amudarya River delta; KP: Karakalpakistan Province of Uzbekistan; TH: Tashauz Province of Turkmenistan; KZ: Khorezm Province of Uzbekistan.

from 1990 to 2000, while it increased by 439.31 $km^2$ from 2000 to 2015. The decrease in sparse vegetation was especially concentrated in the southwestern part of Tashauz Province, while an increase in sparse vegetation was found in the northern part of the AD, indicating land degradation in this region. Built-up land was scattered in croplands and continued to increase from 1696.60 $km^2$ in 1990 to 2600.76 $km^2$ in 2015. The wetland area decreased by 556.06 $km^2$ between 1990 and 2000. However, although the wetland area increased by 341.29 $km^2$ in 2015, the wetland area after 2000 was smaller than that in 1990. Overall, the degree of land use change in croplands and grasslands was higher than that in the other land use types.

The spatial patterns of the land cover change and the changes in the corresponding areas between each time interval are displayed in Figs. 7 and 8, respectively. The land use conversions varied among the three provinces. Throughout the study period, grasslands were the main source of cropland expansion, followed by sparse vegetation. A total of 1135.36 $km^2$ of sparse vegetation in Tashauz Province and 1658.84 $km^2$ of grasslands in Karakalpakistan and Tashauz Provinces were transformed into croplands. Although increased croplands could be beneficial for increasing vegetation greenness, the excessive exploitation of agricultural water resulted in a reduction in ecological water, leading to land degradation in the downstream regions. Additionally, 981.24 $km^2$ of grasslands and 183.10 $km^2$ of croplands were degraded to sparse vegetation in Karakalpakistan Province. Moreover, 920.75 $km^2$ of cropland was abandoned to grassland in this region. These land use changes could be forced by land degradation. For different time intervals, although grasslands and sparse vegetation were the main sources of cropland expansion in both time periods, the conversions from 1990 to 2000 were more serious than those from 2000 to 2015. Additionally, 2809.65 $km^2$ of the new croplands came from sparse vegetation and grasslands from 1990 to 2000. In contrast, for 2000–2015, a major portion of the increased sparse vegetation was mainly attributed to cropland and grassland and was higher than that from 1990 to 2000. The high conversion area from croplands to grasslands during this period was observed in Karakalpakistan Province, with an area up to 1112 $km^2$. The conversions among croplands and natural land cover were the main characteristics of land use change in the AD. The abandonment of croplands and land degradation from grasslands to sparse vegetation obviously exhibited a new trend along with current socio-economic development.

### 3.4. Spatiotemporal dynamics in climate conditions

Fig. 9 presents the spatial distribution of precipitation and temperature change for the different time intervals. Precipitation showed different spatiotemporal changes over different time periods. The AD from 1990 to 2000 experienced a decreased change in precipitation, with large decreases found in the northern part, and an increase was observed from 2000 to 2015, with the greatest change being 65.92 mm. Throughout the study period, the increase in precipitation in the southern part was higher than that in the northern part. The temperatures showed a clear upward trend over the different time intervals. Notably, the temperature increases from 1990 to 2000 were higher than those from 2000 to 2015. The changes ranged from 0.40 °C to 0.54 °C. From 1990 to 2015, the temperatures presented a large increase in northern Karakalpakistan, with the greatest change as high as 0.79 °C. Overall, the AD rapidly warmed from 1990 to 2015, especially in the area surrounding the Aral Sea.

### 3.5. Factors affecting land degradation processes

The relative influence of the explanatory factors for land degradation is determined using the BRT model, as shown in Table S3. The BRT model for land degradation during the study period indicated that water withdrawal, precipitation and temperature explained more than half of the variance (Table S3, Supplementary Material), with relative influences up to 25.2%, 22.1% and 13.7%, respectively. Water withdrawal had a major effect on land degradation, followed by precipitation. The joint pairwise interaction plots for water withdrawal and precipitation indicated that land degradation was more likely to occur in areas with decreased water withdrawal ($< -0.02\ km^3$) and increased precipitation ($< 20$ mm) (Fig. 10). The relative effects of the explanatory factors varied between different vegetation types. The water withdrawal (23.8%) and temperature (15.8%) in croplands were the major driving factors affecting land degradation. In contrast, the precipitation (28%) and temperature (22.3%) in grasslands had major

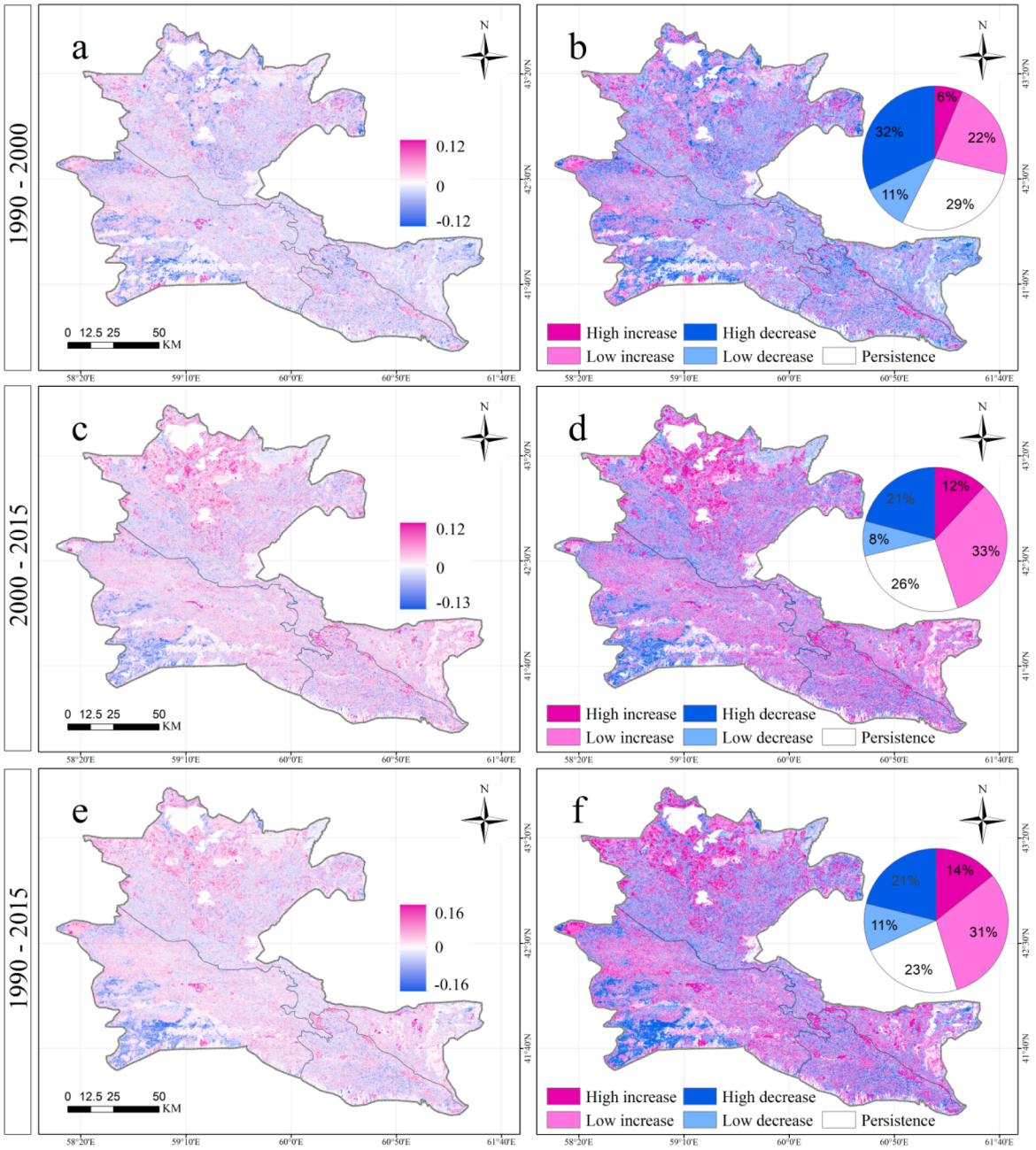


**Fig. 6.** Spatial distribution of soil salinization from 1990 to 2015. (a), (c) and (e) spatial distribution of salinity index (SI) changes between different periods; (b), (d) and (f) intensity of change divided into five classes: low increase, high increase, persistence, low decrease and high decrease.

effects on land degradation. Land degradation in sparse vegetation was driven by several main factors, including precipitation, temperature and livestock, which contributed 27.1%, 22.1% and 16.1%, respectively.

The BRT model for land degradation for 1990–2000 showed that the areas in which precipitation, water withdrawal and salt discharge contributed together equalled almost 70% of the model's explained variance (Table S3, Supplementary Material). Precipitation had a major effect on land degradation during this period. The joint pairwise interaction plot for precipitation and water withdrawal indicated that land degradation was more likely to occur in areas with decreased precipitation ($< -40$ mm) and water withdrawal ($< -0.02$ km$^3$) (Fig. 10). For different vegetation types, water withdrawal (30.2%) and precipitation (25.3%) in croplands constituted the major effects on land degradation. However, grasslands and sparse vegetation with decreased precipitation and increased temperature all contributed to more than half of the model's explained variance for land degradation. For 2000–2015, we found that salt discharge, water withdrawal and precipitation explained more than 50% of the model's explained variance (Table S3, Supplementary Material). Salt discharge (18.1%) showed a major influence on land degradation during this period. The joint pairwise interaction plot for salt discharge and water withdrawal indicated that land degradation was most likely in areas where increased salt discharge to the field plot ($> 40{,}000$ tons) and reduced water withdrawal ($< 0$ km$^3$) occurred (Fig. 10). In croplands, land degradation was mainly explained by salt discharge and water withdrawal, which demonstrated relative influences as high as 26.9% and 18.1%, respectively. In grasslands and sparse vegetation, in addition to the effects of precipitation and temperature, salt discharge contributed to almost 20% of the variance in land degradation. Overall, water

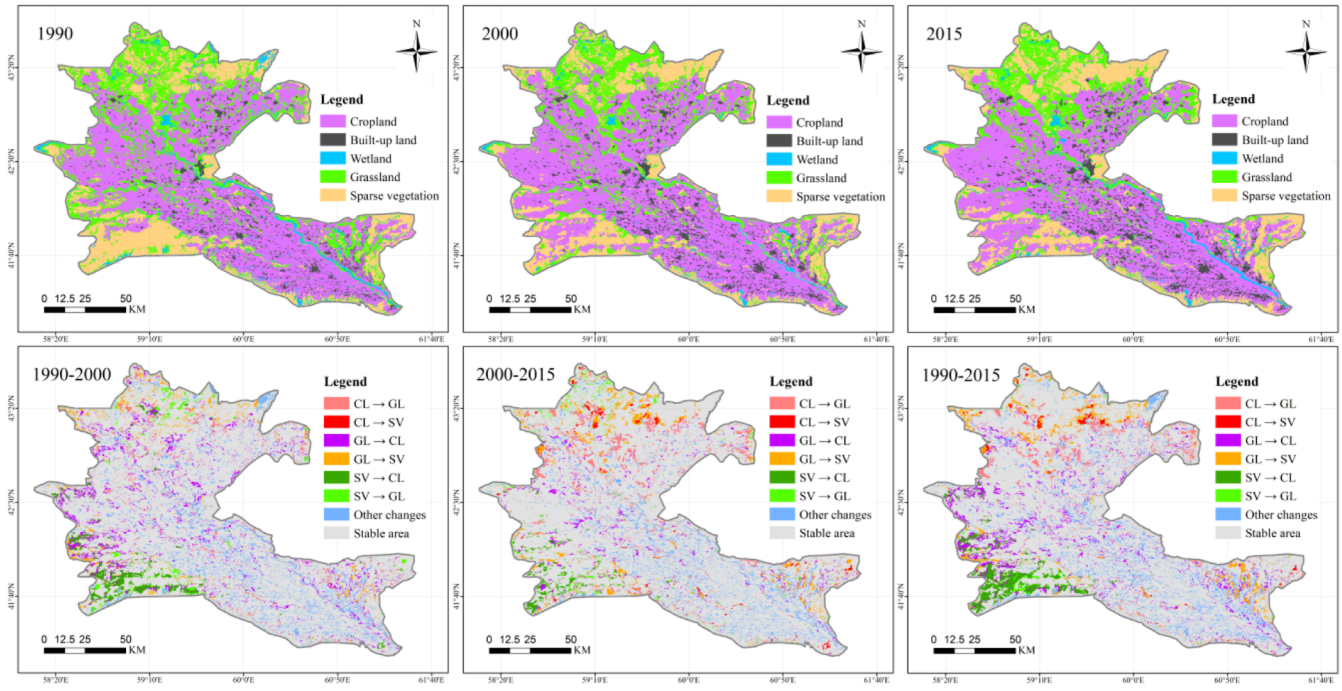


**Fig. 7.** Land use change maps from 1990 to 2015. CL: cropland; GL: grassland; SV: sparse vegetation.

**Table 2**
Statistical areas and percentages of different land use types.

| Type | 1990 | | 2000 | | 2015 | |
|---|---|---|---|---|---|---|
| | $km^2$ | % | $km^2$ | % | $km^2$ | % |
| Cropland | 17583.56 | 48.14 | 19409.96 | 53.14 | 18535.53 | 50.74 |
| Grassland | 8165.73 | 22.35 | 6547.61 | 17.92 | 6313.05 | 17.28 |
| Wetland | 1397.38 | 3.83 | 841.32 | 2.30 | 1182.61 | 3.24 |
| Built-up land | 1696.60 | 4.64 | 2272.35 | 6.22 | 2600.76 | 7.12 |
| Sparse vegetation | 7685.47 | 21.04 | 7457.51 | 20.42 | 7896.82 | 21.62 |

withdrawal, climatic factors and salt discharge had larger impacts on land degradation than other factors in the AD.

According to the salt discharge recorded by the Tyuyamuyun gauging station at the entrance to the AD, the salt discharge increased by 17,108 thousand tons from 2000 to 2015, and the salt discharge to the field plot greatly increased during this time period (Fig. S4, Supplementary Material). The increased salt discharge to the land was a driving factor that could exacerbate soil salinization in the AD. In contrast, a significant decreasing trend in the salt discharge was found before 2000, and the salt discharge to the field plot decreased by 10,204.2 thousand tons. Thus, soil salinization could be alleviated under decreased salt discharge to the field plot. Additionally, based on the observation data recorded at the well near the Aral Sea, the annual change in groundwater tables changed dramatically throughout the study period. A considerable drop and rise in the groundwater table were observed before and after 2001, respectively. The changes in the groundwater table inevitably impacted the soil salinization in this region. Therefore, the overall changes in soil salinization were closely correlated with the salt discharge and groundwater tables. This phenomenon may be caused by human activities in this region.

## 4. Discussion

### 4.1. Anthropogenic disturbances of land degradation

The directions of land degradation of different vegetation types for different time intervals were investigated in this research. Previous studies focused on land degradation based on the change trend of vegetation indicators, which ignored land use change. The effects of land degradation could not be detected effectively (Zhang et al., 2017). Land degradation is the result of a combination of drivers (D'Odorico et al., 2013). Thus, the main driving factors of land degradation were evaluated over different time intervals based on the BRT model. The combination of the BRT model and land degradation constituted another technical advancement in this type of research.

Water withdrawal for 1990–2000 was the most influential factor explaining the land degradation of croplands in the AD (Table S3, Supplementary Material). Many croplands were distributed in this region and were irrigated with river water. However, after 1990, dry spells were frequently observed (Stulina and Eshchanov, 2013). Decreased runoff in the AD was observed from 1990 to 2000 and attributed to climate change and excessive water withdrawal in the upstream regions (Fig. S5a, Supplementary Material), and the agricultural water availability was greatly reduced. Decreases in water withdrawal of 57.64%, 38.04% and 28.30% were recorded in Karakalpakistan, Khorezm and Tashauz Provinces from 1990 to 2000, respectively, and a severe agricultural water shortage occurred in 2000, especially in Karakalpakistan Province (Figs. S5b–d, Supplementary Material). Furthermore, due to the agricultural expansion in the southwestern part of Tashauz Province, a water supply canal was built on the left bank of the Tyuyamuyun reservoir and connected to the Malyab Canal. Together, they are known as Turkmen Darya, which delivers water from the Amudarya River (Zonn and Kostianoy, 2013). Thus, we found that most of the cropland expansion converted from sparse vegetation was concentrated in this region (Figs. 7 and 8). The area of croplands increased by 1826.40 $km^2$ during this period (Table 2). Subsequently, the agricultural water shortages were further exacerbated, especially in the downstream area of Karakalpakistan Province (Fig. S5b, Supplementary Material). As the water use per irrigated area decreased, the soil moisture levels were reduced, and the croplands were susceptible to droughts, resulting in land degradation and major crop failures (Dubovyk et al., 2013a; Kulmatov, 2014). The results of the present study confirm that the proportion of land degradation was higher than the amount of land improvement in this period. Additionally, land

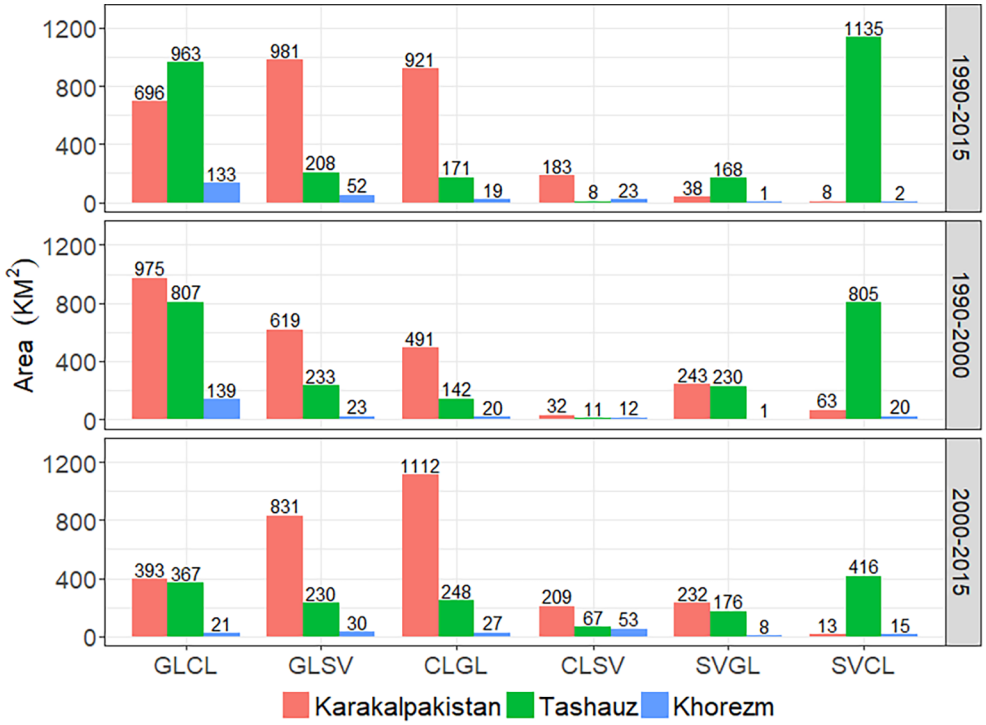


**Fig. 8.** Land use change in areas between each time interval. GLCL: grassland to cropland; GLSV: grassland to sparse vegetation; CLGL: cropland to grassland; CLSV: cropland to sparse vegetation; SVGL: sparse vegetation to grassland; SVCL: sparse vegetation to cropland.

degradation in the downstream areas was more serious than that in the upstream regions (Fig. 5).

Salt discharge to the field plot showed a major influence on land degradation in croplands from 2000 to 2015 (Table S3, Supplementary Material). Thus, severe soil salinization was observed in most of the regions during this period, especially in Khorezm and northern Karakalpakistan (Fig. 6). In Khorezm, most subsoils are slightly or moderately saline, while most topsoils above 60 cm are strongly saline (Akramkhanov et al., 2012). The water withdrawal in Khorezm increased by 53.03% from 2000 to 2015 (Fig. S5, Supplementary Material). Approximately 62% of the irrigation water withdrawal was wasted before being used in crops because of the low irrigation efficiency (Kitamura et al., 2006). Furthermore, the drainage network has limited capacity. This water waste caused a rise in the groundwater level to 1.5 m as well as an increase in groundwater salinization during the cropping season (Fig. S4b, Supplementary Material) (Stulina and

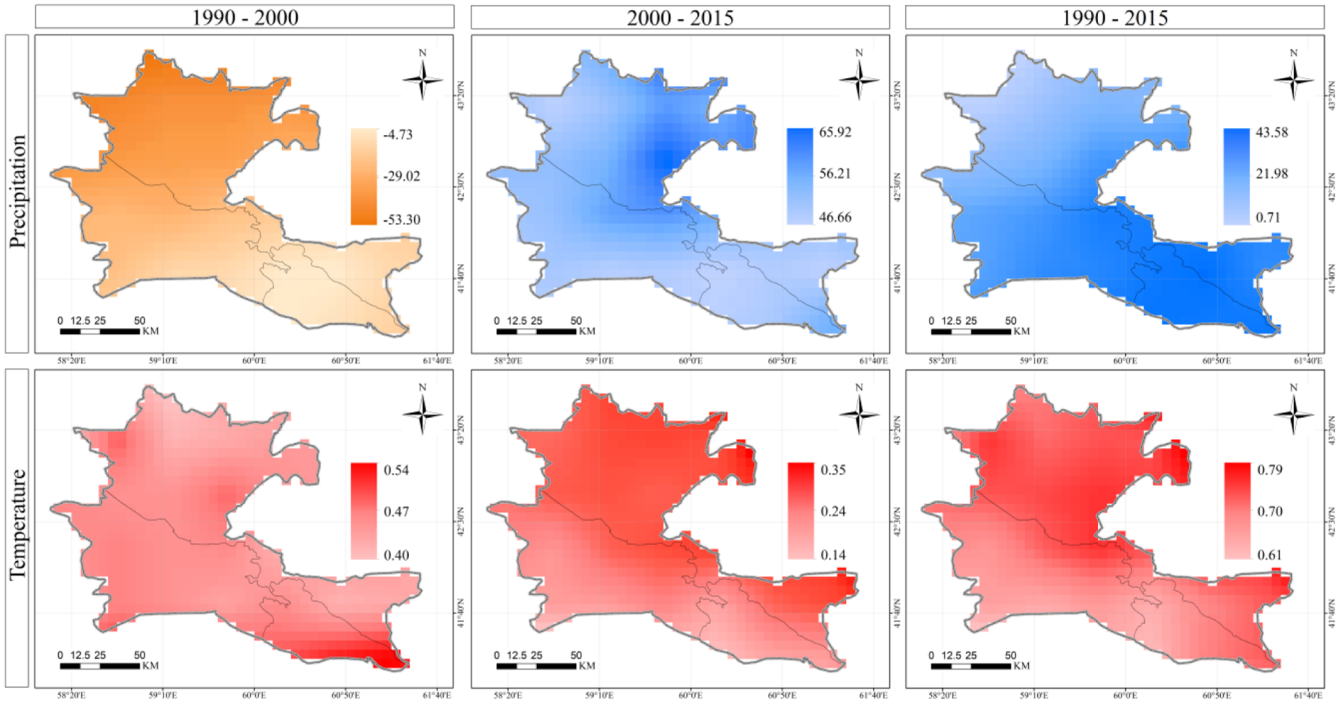


**Fig. 9.** Spatial distribution of precipitation and temperature change between different periods.

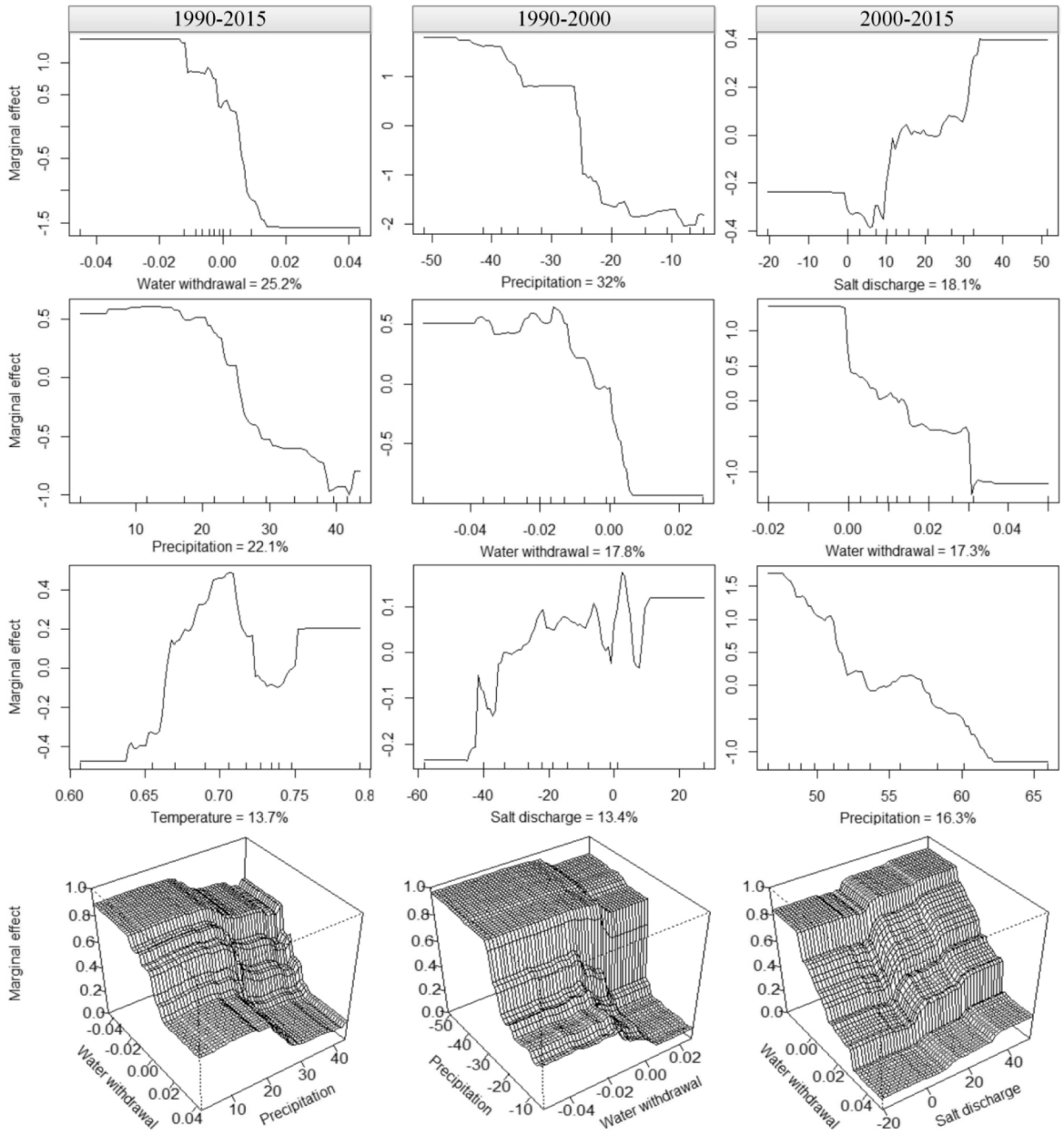


**Fig. 10.** Partial dependence plots for the three relative importance values for the explanatory factors in the BRT model. The horizontal axis includes rug plots that display the distribution of the influential factors in percentiles. The vertical axis shows the marginal effect along the explanatory factors.

Eshchanov, 2013). Therefore, secondary soil salinization is particularly serious in the arable lands of Khorezm Province. The salinization of secondary soil mainly resulted from the salinity of irrigation water and groundwater (Ibrakhimov et al., 2007). Moreover, much of the irrigation water from the upstream regions of the river flowed into the northern part of Karakalpakistan (Severskiy, 2004). The salt discharge to croplands largely increased by 8228.2 thousand tons during this time period (Fig. S4a, Supplementary Material), and was more serious in the downstream areas than in the upstream areas. Thus, many croplands experienced large increases in salinization (Fig. 6), and some croplands were abandoned to grasslands and sparse vegetation in northern Karakalpakistan (Fig. 7). Additionally, after the Soviet Union collapsed, Turkmenistan and Uzbekistan changed from a socialist to a capitalist society, resulting in massive rural-urban migration and a different economic development model as planned economies transitioned towards free markets (Gleason, 2003). Subsequently, the heavy subsidy for agriculture disappeared, and agriculture was characterized by a substantial decline in profitability and insecure land tenure (Hostert et al., 2011). This difference facilitated the abandonment of degraded croplands in the AD. Simultaneously, abandonment of farmlands also caused adverse socio-economic impacts, including increased food insecurity, reduced households and increased unemployment (Bekchanov and Lamers, 2016).

Most grasslands and sparse vegetation were distributed in the northern part of the AD. The result of the BRT model indicated that salt discharge was a major force causing land degradation from 2000 to 2015. Although the increased precipitation was beneficial for vegetation growth (Fig. 10), increased sparse vegetation was found because of the conversion of grassland near the Aral Sea (Figs. 7 and 8). In addition to the effects of groundwater salinization, increased salinity in river runoff was noticed from 2000 to 2015. According to the data on salt discharge recorded by the Samanbay gauging station (near the Aral Sea), the salt discharge increased during this period (Fig. S4a, Supplementary Material). The northern part of the AD received a large

amount of saltwater, which contributed to severe soil salinization of grasslands and sparse vegetation, which were widely distributed in this region that experienced land degradation (Fig. 6). This observation explains the fact that the regions have been degraded with increased precipitation (Figs. 7 and 10). Soil salinization in most regions was more serious from 2000 to 2015 than from 1990 to 2000, particularly in the northern AD (Fig. 6).

### 4.2. Climate change as a driver of land degradation

The BRT model showed that precipitation and temperature were the main driving factors affecting the land degradation of grasslands and sparse vegetation (Table S3, Supplementary Material). The growth of natural vegetation is not dependent on artificial irrigation. Rather, the growth is dependent on rainfall. We found that precipitation in the AD experienced an overall decreasing trend from 1990 to 2000 (Fig. 9, Supplementary Material) and that a strong negative relationship existed between the marginal effect of land degradation and precipitation (Fig. 10).

The previous finding indicated that water withdrawal was related to the change in water resources during the study period in the Aral Sea basin. As presented in Fig. S6, the annual runoff varies strongly because of climate change in the mountains. The correlation coefficients between runoff and precipitation and temperature were 0.53 and −0.47, respectively. Therefore, the large climatic fluctuations in the mountains were also a driver of the runoff change and affected the water available for withdrawal and soil salinization in the Aral Sea basin. Furthermore, the relationship between river flow and ecological water was positive, with a correlation coefficient as high as 0.96 (Fig. S5a, Supplementary Material). Thus, climate change could have influenced the availability of water for the ecological environment in the AD, especially from 1990 to 2000. The decreased amount of ecological water has caused grassland degradation in some areas near the former shoreline. This observation indicates that significant land degradation was observed in the transitions among grasslands and sparse vegetation in the northern part of the AD (Figs. 7 and 8). Therefore, this region experienced significant land degradation as a result of the severe reduction in river inflows during 1990–2000 (Asarin et al., 2010). Throughout the study area, land degradation in the downstream areas from 1990 to 2000 was more serious than that in the upstream areas.

In addition, the Aral Sea has steadily declined in size primarily due to expanding irrigation after 1960 (Micklin, 2007). However, the agricultural water tended to remain in the upstream regions after 1990 (Micklin et al., 2016a). The dramatic decrease in the river inflow generated from the Pamir and Hindukush mountains contributed to the accelerated recession of the Aral Sea (Fig. S6b, Supplementary Material). The large Aral Sea was separated into its eastern and western parts in 2006. Furthermore, the area of the Aral Sea shrunk to nearly 0 in 2014. As the dryness in summer strengthened, the continental climate changed, which led to a significant increase in evaporation from plants (Micklin et al., 2016b). Thus, more land areas surrounding the Aral Sea exhibited high land degradation than in other regions (Fig. 4). This result is consistent with a previous study indicating that some fields near the Aral Sea became highly sensitive to desertification during this period (Jiang et al., 2019).

Identifying areas with land degradation can play a supporting role in the implementation of the land degradation neutrality (LDN) initiative (Prăvălie et al., 2017). The LDN initiative proposes that the quality of land resources should remain stable or increase. Sustainable Development Goal 15 specifically called for achieving the LDN initiative by the year 2030 (Wunder et al., 2018). The results of factors affecting land degradation suggest several practical measures for reducing land degradation in the downstream areas: (1) application of drip irrigation in agricultural areas, which can reduce evaporation and drainage losses; (2) restriction of the expansion of irrigated lands, especially in southwestern Tashauz Province; (3) reduction in salt discharge from the upstream regions; and (4) assurance of a suitable groundwater table for vegetation growth. Additionally, the stable land areas should maintain their current state via the implementation of appropriate measures in the AD. A previous study indicated that land degradation undermined ecosystem functions and services and has negative effects on ecological and socio-economic systems (Prăvălie et al., 2017). Therefore, identifying areas with land degradation as the main spatial targets for the deployment of restoration plans is critical for the implementation of the LDN initiative.

## 5. Conclusions

This research monitored the land degradation in the AD by applying CVA to NDVI and albedo for the period of 1990–2015. By linking the trajectories of land use change, we investigated land degradation and calculated the relative importance of the driving factors for land degradation based on the BRT model. The results illustrated that land degradation was especially concentrated in the downstream areas of northern Karakalpakistan throughout the study period (1990–2015), with magnitude values amounting to 0.38. In contrast, land improvements were observed in the southwestern part of Tashauz Province, with magnitude values as low as −0.38. Some land areas gradually degraded and were categorized as high land degradation in the AD, especially in the downstream areas surrounding the Aral Sea.

Land degradation could force land use changes in the AD. Transitions among natural vegetation and croplands are major features of contemporary land use change in this region. Severe land degradation was detected in many regions, especially in northern Karakalpakistan Province. Subsequently, 920.75 $km^2$ and 183.10 $km^2$ of abandoned croplands have been converted to sparse vegetation and grasslands, respectively, and have suffered from severe land degradation in northern Karakalpakistan Province. Moreover, 981.24 $km^2$ of grassland has degraded into sparse vegetation. As the vegetation cover of different land use types increases, the extent of the influence of land degradation will increase in the AD.

Land degradation over different time intervals was caused by several major driving factors. From 1990 to 2000, the water available for withdrawal was the most influential factor explaining the land degradation of croplands. The agricultural water availability was greatly reduced during dry spells. Furthermore, much of the sparse vegetation in southwestern Tashauz Province was reclaimed as arable lands. Subsequently, agricultural water shortages were exacerbated in Karakalpakistan. Decreased precipitation was the main driving factor that affected the land degradation of sparse vegetation and grasslands. The growth of natural vegetation is not dependent on artificial irrigation but rather on rainfall. The BRT model indicated that land degradation was more likely to appear in areas with decreased precipitation (< −40 mm) and water withdrawal (< −0.02 $km^3$).

In contrast, salt discharge to the field plot was the main force that caused land degradation of croplands in the AD over the subsequent time interval of 2000–2015. A rise in the groundwater level in this period was observed to cause problems in the use of water resources, resulting in secondary soil salinization and land degradation. For grasslands and sparse vegetation, the increases in salt discharge from upstream regions contributed to severe soil salinization in the natural vegetation, which contributed to land degradation. The BRT model indicated that land degradation was most noticeable in areas with increased salt discharge to the field plot (> 40 thousand tons) and reduced water withdrawal (< 0 $km^3$). Notably, because of the continued shrinkage of the Aral Sea, some lands surrounding the sea have experienced high land degradation.

Our findings can contribute to the implementation of the LDN initiative in the AD. The identification of areas with land degradation in the downstream areas can be used as the main spatial targets for the implementation of the LDN initiative to deploy restoration plans. In addition, it is extremely important to keep the stable regions identified

in this study in their current state. Land degradation results from a combination of multiple factors and is an extremely complex changing process. Due to the availability of data on the explanatory factors, we did not consider other impacts on land degradation. In future studies, more explanatory factors are needed to obtain a deeper understanding of land degradation in the AD.

## Author contributions

Anming Bao designed the research. Liangliang Jiang processed the data, analyzed the results and wrote the manuscript. Guli·Jiapaer, Hao Guo, Guoxiong Zheng and Philippe De Maeyer provided the analysis tools and technical assistance. All authors contributed to the final version of the manuscript by their proofreading and by offering constructive ideas.

## Declaration of Competing Interest

The authors declare that they have no known competing financial interests or personal relationships that could have appeared to influence the work reported in this paper.

## Acknowledgements

We would like to thank the Interstate Commission for Water Coordination of Central Asia for sharing some hydrological data and water use data in the AD. We thank Research Centre for Ecology and Environment of Central Asia for sharing the land use data. We also acknowledge the Climatic Research Unit (University of East Anglia) for providing data on the gridded climate data (the Climatic Research Unit Version 4.01) from their website at http://www.cru.uea.ac.uk/data/. This research has been supported by the Strategic Priority Research Program of Chinese Academy of Sciences [Grant No. XDA19030301], China and Tianshan Innovation Team Project of the Xinjiang Department of Science and Technology [Grant No. Y744261], China.

## Appendix A. Supplementary data

Supplementary data to this article can be found online at https://doi.org/10.1016/j.ecolind.2019.105595.

## References

Akhtar, F., Tischbein, B., Awan, U.K., 2013. Optimizing deficit irrigation scheduling under shallow groundwater conditions in lower reaches of amu darya River Basin. Water Resourc. Manage. 27, 3165–3178.
Akramkhanov, A., Kuziev, R., Sommer, R., Martius, C., Forkutsa, O., Massucati, L., 2012. Soils and soil ecology in Khorezm. Cotton Water Salts Soums 37–58.
Asarin, A.E., Kravtsova, V.I., Mikhailov, V.N., 2010. Amudarya and Syrdarya Rivers and Their Deltas. Springer, Berlin Heidelberg.
Bandoc, G., Prăvălie, R., 2015. Climatic water balance dynamics over the last five decades in Romania's most arid region, Dobrogea. J. Geogr. Sci. 25, 1307–1327.
Bank, T.W., 1998. Aral Sea Basin Program. Water and Environmental Management Project, (Kazakhstan, Kyrgyz Republic, Tajikistan, Turkmenistan and Uzbekistan).
Bekchanov, M., Lamers, J.P.A., 2016. Economic costs of reduced irrigation water availability in Uzbekistan (Central Asia). Regional Environ. Change 16, 2369–2387.
Bouaziz, M., Matschullat, J., Gloaguen, R., 2011. Improved remote sensing detection of soil salinity from a semi-arid climate in Northeast Brazil. Comptes. Rendus Geosci. 343, 795–803.
Chen, X., Luo, G., Wu, S., Wang, W., Fang, H., Chen, Q., 2015. Land Use/Cover Change in Arid Land of Central Asia. Science Press.
Conrad, C., Dech, S., Dubovyk, O., Fritsch, S., Klein, D., Löw, F., Schorcht, G., Zeidler, J., 2014. Derivation of temporal windows for accurate crop discrimination in heterogeneous croplands of Uzbekistan using multitemporal RapidEye images. Comput. Electr. Agric. 103, 63–74.
D'Odorico, P., Bhattachan, A., Davis, K.F., Ravi, S., Runyan, C.W., 2013. Global desertification: drivers and feedbacks. Adv. Water Resourc. 51, 326–344.
Dawelbait, M., Morari, F., 2012. Monitoring desertification in a Savannah region in Sudan using Landsat images and spectral mixture analysis. J. Arid Environ. 80, 45–55.
Dubovyk, O., Menz, G., Conrad, C., Kan, E., Machwitz, M., Khamzina, A., 2013a. Spatio-temporal analyses of cropland degradation in the irrigated lowlands of Uzbekistan using remote-sensing and logistic regression modeling. Environ. Monitor. Assess 185, 4775–4790.
Dubovyk, O., Menz, G., Conrad, C., Lamers, J.P.A., Lee, A., Khamzina, A., 2013b. Spatial targeting of land rehabilitation: a relational analysis of cropland productivity decline in arid Uzbekistan. Erdkunde 67, 167–181.
Dubovyk, O., Menz, G., Khamzina, A., 2016. Land Suitability assessment for afforestation withelaeagnus Angustifolial. in Degraded agricultural areas of the lower amudarya River Basin. Land Degr. Dev. 27, 1831–1839.
Elith, J., Leathwick, J.R., Hastie, T., 2008. A working guide to boosted regression trees. J. Animal Ecol. 77, 802–813.
Friedman, J.H., 2001. Greedy function approximation: a gradient boosting machine. Ann. Statistics 1189–1232.
Friedman, J.H., 2002. Stochastic gradient boosting. Comput. Stat. Data Anal. 38, 367–378.
Gebremicael, T.G., Mohamed, Y.A., van der Zaag, P., Hagos, E.Y., 2018. Quantifying longitudinal land use change from land degradation to rehabilitation in the headwaters of Tekeze-Atbara Basin, Ethiopia. Sci. Total Environ. 622–623, 1581–1589.
Gleason, G., 2003. Markets and politics in Central Asia. Routledge.
Gorji, T., Sertel, E., Tanik, A., 2017. Monitoring soil salinity via remote sensing technology under data scarce conditions: a case study from Turkey. Ecol. Indic. 74, 384–391.
Hastie, T., Tibshirani, R., Friedman, J.H., Franklin, J., 2015. The Elements of Statistical Learning.
Hijmans, R.J., Elith, J., 2013. Species distribution modeling with R. R package version 0. 8-11.
Hostert, P., Kuemmerle, T., Prishchepov, A., Sieber, A., Lambin, E.F., Radeloff, V.C., 2011. Rapid land use change after socio-economic disturbances: the collapse of the Soviet Union versus Chernobyl. Environ. Res. Lett. 6, 045201.
Ibrakhimov, M., Khamzina, A., Forkutsa, I., Paluasheva, G., Lamers, J.P.A., Tischbein, B., Vlek, P.L.G., Martius, C., 2007. Groundwater table and salinity: spatial and temporal distribution and influence on soil salinization in Khorezm region (Uzbekistan, Aral Sea Basin). Irrigation Drainage Syst. 21, 219–236.
IPBES, 2018. Intergovernmental Science-Policy Platform on Biodiversity and Ecosystem Services – The Assessment Report on Land Degradation and Restoration. Summary for Policymakers, IPBES secretariat, Bonn, Germany.
Jiang, L., Bao, A., Jiapaer, G., Guo, H., Zheng, G., Gafforov, K., Kurban, A., De Maeyer, P., 2019. Monitoring land sensitivity to desertification in Central Asia: convergence or divergence? Sci. Total Environ. 658, 669–683.
Karnieli, A., Qin, Z., Wu, B., Panov, N., Yan, F., 2014. Spatio-temporal dynamics of land-use and land-cover in the Mu Us Sandy Land, China, using the change vector analysis technique. Remote Sens. 6, 9316–9339.
Khamzina, A., Lamers, J.P.A., Vlek, P.L.G., 2008. Tree establishment under deficit irrigation on degraded agricultural land in the lower Amu Darya River region, Aral Sea Basin. Forest Ecol. Manage. 255, 168–178.
Kitamura, Y., Yano, T., Honna, T., Yamamoto, S., Inosako, K., 2006. Causes of farmland salinization and remedial measures in the Aral Sea basin – research on water management to prevent secondary salinization in rice-based cropping system in arid land. Agric. Water Manage. 85, 1–14.
Kulmatov, R., 2014. Problems of sustainable use and management of water and land resources in Uzbekistan. J. Water Resour. Protect. 06, 35–42.
Kundu, A., Dutta, D., 2011. Monitoring desertification risk through climate change and human interference using remote sensing and GIS techniques. Int. J. Geomat. Geosci. 2, 21–33.
Lal, R., Suleimenov, M., Stewart, B., Hansen, D., Doraiswamy, P., 2007. Climate Change and Terrestrial Carbon Sequestration in Central Asia. CRC Press.
Lambin, E.F., Strahlers, A.H., 1994. Change-vector analysis in multitemporal space: a tool to detect and categorize land-cover change processes using high temporal-resolution satellite data. Remote Sens. Environ. 48, 231–244.
Lee, S.O., Jung, Y., 2018. Efficiency of water use and its implications for a water-food nexus in the Aral Sea Basin. Agric. Water Manage. 207, 80–90.
Li, Q., Zhang, C., Shen, Y., Jia, W., Li, J., 2016. Quantitative assessment of the relative roles of climate change and human activities in desertification processes on the Qinghai-Tibet Plateau based on net primary productivity. Catena 147, 789–796.
Liang, S., 2001. Narrowband to broadband conversions of land surface albedo I: algorithms. Remote Sens. Environ. 76, 213–238.
Liu, F., Chen, Y., Lu, H., Shao, H., 2017. Albedo indicating land degradation around the Badain Jaran Desert for better land resources utilization. Sci. Total Environ. 578, 67–73.
Liu, Q., Zhao, Y., Zhang, X., Buyantuev, A., Niu, J., Wang, X., 2018. Spatiotemporal patterns of desertification dynamics and desertification effects on ecosystem services in the Mu Us Desert in China. Sustainability 10, 589.
Ma, Z., Xie, Y., Jiao, J., Li, L., Wang, X., 2011. The construction and application of an Aledo-NDVI based desertification monitoring model. Procedia Environ. Sci. 10, 2029–2035.
Mann, H.B., 1945. Nonparametric tests against trend. Econometrica 13, 245–259.
Mariano, D.A., Santos, C.A.C.D., Wardlow, B.D., Anderson, M.C., Schiltmeyer, A.V., Tadesse, T., Svoboda, M.D., 2018. Use of remote sensing indicators to assess effects of drought and human-induced land degradation on ecosystem health in Northeastern Brazil. Remote Sens. Environ. 213, 129–143.
Micklin, P., 2004. The Aral Sea crisis, Dying and Dead Seas Climatic Versus Anthropic Causes. Springer, pp. 99–123.
Micklin, P., 2007. The Aral sea disaster. Annu. Rev. Earth Planet. Sci. 35, 47–72.
Micklin, P., Aladin, N.V., Plotnikov, I., 2016a. Aral Sea. Springer.
Micklin, P., Aladin, N.V., Plotnikov, I., 2016b. The Aral Sea. Springer.
Mitchell, T.D., Jones, P.D., 2005. An improved method of constructing a database of monthly climate observations and associated high-resolution grids. Int. J. Climatol. 25, 693–712.

Müller, D., Leitão, P.J., Sikor, T., 2013. Comparing the determinants of cropland abandonment in Albania and Romania using boosted regression trees. Agric. Syst. 117, 66–77.
Naghibi, S.A., Pourghasemi, H.R., Dixon, B., 2016. GIS-based groundwater potential mapping using boosted regression tree, classification and regression tree, and random forest machine learning models in Iran. Environ. Monitor. Assess. 188, 44.
Pan, J., Li, T., 2013. Extracting desertification from Landsat TM imagery based on spectral mixture analysis and Albedo-Vegetation feature space. Natural Hazards 68, 915–927.
Prăvălie, R., 2016. Drylands extent and environmental issues. A global approach. Earth-Sci. Rev. 161, 259–278.
Prăvălie, R., Bandoc, G., Patriche, C., Sternberg, T., 2019a. Recent changes in global drylands: evidences from two major aridity databases. Catena 178, 209–231.
Prăvălie, R., Bandoc, G., Patriche, C., Tomescu, M., 2016. Spatio-temporal trends of mean air temperature during 1961–2009 and impacts on crop (maize) yields in the most important agricultural region of Romania. Stochastic Environ. Res. Risk Assess. 31, 1923–1939.
Prăvălie, R., Patriche, C., Bandoc, G., 2017. Quantification of land degradation sensitivity areas in Southern and Central Southeastern Europe. New results based on improving DISMED methodology with new climate data. Catena 158, 309–320.
Prăvălie, R., Piticar, A., Roșca, B., Sfîcă, L., Bandoc, G., Tiscovschi, A., Patriche, C., 2019b. Spatio-temporal changes of the climatic water balance in Romania as a response to precipitation and reference evapotranspiration trends during 1961–2013. Catena 172, 295–312.
Reynolds, J.F., Smith, D.M.S., Lambin, E.F., Turner, B., Mortimore, M., Batterbury, S.P., Downing, T.E., Dowlatabadi, H., Fernández, R.J., Herrick, J.E., 2007. Global desertification: building a science for dryland development. Science 316, 847–851.
Röder, A., Hill, J., 2009. Recent Advances in Remote Sensing and Geoinformation Processing for Land Degradation Assessment. CRC Press.
Rouse Jr, J.W., Haas, R., Schell, J., Deering, D., 1974. Monitoring vegetation systems in the Great Plains with ERTS.
Saiko, T.A., Zonn, I.S., 2000. Irrigation expansion and dynamics of desertification in the Circum-Aral region of Central Asia. Appl. Geogr. 20, 349–367.
Salih, A.A.M., Ganawa, E.T., Elmahl, A.A., 2017. Spectral mixture analysis (SMA) and change vector analysis (CVA) methods for monitoring and mapping land degradation/desertification in arid and semiarid areas (Sudan), using Landsat imagery. Egypt. J. Remote Sens. Space Sci.
Schapire, R.E., 2003. The Boosting Approach to Machine. Learning: An Overview.
Schettler, G., Oberhänsli, H., Stulina, G., Mavlonov, A.A., Naumann, R., 2013. Hydrochemical water evolution in the Aral Sea Basin. Part I: unconfined groundwater of the Amu Darya Delta – interactions with surface waters. J. Hydrol. 495, 267–284.
Schlüter, M., Khasankhanova, G., Talskikh, V., Taryannikova, R., Agaltseva, N., Joldasova, I., Ibragimov, R., Abdullaev, U., 2013. Enhancing resilience to water flow uncertainty by integrating environmental flows into water management in the Amudarya River, Central Asia. Global Planetary Change 110, 114–129.
Severskiy, I.V., 2004. Water-related problems of Central Asia: some results of the (GIWA) international water assessment program. Ambio 52–62.
Sica, Y.V., Quintana, R.D., Radeloff, V.C., Gavier-Pizarro, G.I., 2016. Wetland loss due to land use change in the Lower Parana River Delta, Argentina. Sci. Total Environ. 568, 967–978.
Sneyers, R., 1991. On the statistical analysis of series of observations.
Stulina, G., Eshchanov, O., 2013. Climate change impacts on hydrology and environment in the Pre-Aral region. Quarter. Int. 311, 87–96.
Su, S., Xiao, R., Li, D., Hu, Y., 2014. Impacts of transportation routes on landscape diversity: a comparison of different route types and their combined effects. Environ. Manage 53, 636–647.
UNCCD, 1994. United Nations Convention to Combat Desertification in those countries experiencing serious drought and/or desertification, particularly in Africa, Paris, France.
UNCCD, 2017. United Nations Convention to Combat Desertification – Global land outlook UNCCD secretariat, Bonn, Germany.
Vogt, J.V., Safriel, U., Von Maltitz, G., Sokona, Y., Zougmore, R., Bastin, G., Hill, J., 2011. Monitoring and assessment of land degradation and desertification: towards new conceptual and integrated approaches. Land Degr. Dev. 22, 150–165.
Vorovencii, I., 2017. Applying the change vector analysis technique to assess the desertification risk in the south-west of Romania in the period 1984–2011. Environ. Monitor. Assess. Cambridge, UK 189, 524.
White, K.D., 2013. Nature–society linkages in the Aral Sea region. J. Eurasian Stud. 4, 18–33.
Wunder, S., Kaphengst, T., Frelih-Larsen, A., 2018. Implementing land degradation neutrality (SDG 15.3) at national level: general approach, indicator selection and experiences from Germany. In: International Yearbook of Soil Law and Policy 2017. Springer, pp. 191–219.
Zaady, E., Karnieli, A., Shachak, M., 2007. Applying a field spectroscopy technique for assessing successional trends of biological soil crusts in a semi-arid environment. J. Arid Environ. 70, 463–477.
Zhang, G., Biradar, C.M., Xiao, X., Dong, J., Zhou, Y., Qin, Y., Zhang, Y., Liu, F., Ding, M., Thomas, R.J., 2017. Exacerbated grassland degradation and desertification in Central Asia during 2000–2014. Ecol. Appl. 28.
Zhou, W., Gang, C., Zhou, F., Li, J., Dong, X., Zhao, C., 2015. Quantitative assessment of the individual contribution of climate and human factors to desertification in northwest China using net primary productivity as an indicator. Ecol. Indic. 48, 560–569.
Zonn, I.S., Kostianoy, A.G., 2013. The Turkmen Lake Altyn Asyr and Water Resources in Turkmenistan. Springer.